Lepton energy asymmetry and precision supersymmetry study at hadron colliders

Nojiri, MM; Toya, D; Kobayashi, T

PHYSICAL REVIEW D, VOLUME 62, 075009

Lepton energy asymmetry and precision supersymmetry study at hadron colliders

Mihoko M. Nojiri
YITP, Kyoto University, Kyoto 606-8502, Japan

Daisuke Toya and Tomio Kobayashi
ICEPP, Universiy of Tokyo, Hongo, Bunkyo, Tokyo 113-0033, Japan

(Received 27 January 2000; published 12 September 2000)

We study the distribution of lepton pairs from the second lightest neutralino decay $\tilde{\chi}_2^0 \to \tilde{l} l$ followed by $\tilde{l} \to \tilde{\chi}_1^0 l$. The distribution of the ratio of lepton transverse momenta A_T shows a peak structure if $m_{ll} \lesssim m_{ll}^{\max}/2$ is required. The peak position $A_T^{\rm peak}$ is described by a simple function of the gaugino and slepton masses in the $m_{ll} \sim 0$ limit. When a moderate m_{ll} cut is applied, the $A_T^{\rm peak}$ depends on the $\tilde{\chi}_2^0$ velocity distribution, but the dependence would be corrected by studying the lepton P_T distribution. $A_T^{\rm peak}$ and the edge of m_{ll} distributions are used to determine the mass parameters involved in the decay for parameters of interest to CERN Large Hadron Collider experiments. For some cases the gaugino and slepton masses may be determined within 10% by the lepton distribution only independent of model assumptions. Correct combinations of $A_T^{\rm peak}$ and $m_{ll}^{\rm edge}$ would be identified even if different $\tilde{\chi}_2^0$ decay chains are coexisting. The analysis could be extended to the Fermilab Tevatron energy scale or other cascade decays.

PACS number(s): 14.80.Ly, 11.30.Pb, 12.60.Jv

I. INTRODUCTION

The minimal supersymmetric standard model (MSSM) [1] is one of the most promising extensions of the standard model. It offers a natural solution of the hierarchy problem, amazing gauge coupling unification, and dark matter candidates. If nature chooses low energy supersymmetry (SUSY), sparticles will be found *for sure*, as they will be copiously produced at future colliders such as the Large Hadron Collider (LHC) at CERN or TeV scale e^+e^- linear colliders (LC's) proposed by DESY, KEK, and SLAC. LHC would be a great discovery machine. Squarks and gluinos with a mass less than a few TeV would be found unless the decay patterns are noncanonical [2].

On the other hand, the MSSM suffers severe flavor changing neutral current constraints if no mass relation is imposed on sfermion mass parameters [3]. Various proposals have been made for the mechanism to incorporate SUSY breaking in ''our sector,'' trying to offer natural explanations of such mass relations [4]. The discovery of SUSY is not the final goal, but it is the beginning of a new quest for ''the mechanism'' of SUSY breaking.

Measurements of soft breaking masses would be an important aspect of the study of SUSY, because different SUSY breaking mechanisms predict different sparticle mass patterns. Studies at the Fermilab Tevatron and LHC would suffer from substantial uncertainties and backgrounds compared to a LC, such as luminosity error, combinatorial backgrounds, and unknown initial energy. Therefore it is very interesting to see the ultimate precision of supersymmetric studies at the LHC.

It is possible to determine masses of sparticles from the measurement of end points of invariant mass distributions [2,5–7]. For the minimal supergravity (MSUGRA) and gauge mediated models, there was substantial success for the parameter points where the decay of the second lightest neutralino to lepton pair $\tilde{\chi}_2^0 \to l l \tilde{\chi}_1^0$ is detected with substantial statistics. For some cases, one would be able to not only determine all MSUGRA parameters, but also to measure the masses of some sparticles, using the edges and end points of invariant mass distributions involving jets and leptons. The systematic errors of such analyses may be controlled if the acceptance near the end points and (jet) energy resolution are known.

Detailed studies in this direction have been performed, and we do not repeat these here. In this paper, we instead study the ratio of lepton P_T (lepton P_T asymmetry $A_T \equiv P_{T2}^l / P_{T1}^l$; $P_{T2}^l < P_{T1}^l$) for the decay $\tilde{\chi}_2^0 \to \tilde{l} l \to l l \tilde{\chi}_1^0$. The information has been used in previous analyses [5,8] in the context of global fits of MSUGRA parameters. We show that it is possible to make a direct connection between the peak structure of the asymmetry $A_T^{\rm peak}$ and the ratio of the lepton energies in the neutralino rest frame A_E by using events with $m_{ll} < m_{ll}^{\max}/2$. We also point out that systematics due to the $\tilde{\chi}_2^0$ velocity distribution would be small and reduced further if one includes the P_T distribution of the hardest lepton in the fit. Using the m_{ll} end point and the peak position of the A_T distribution, one can at least determine two degrees of freedom of the three parameters involved in the $\tilde{\chi}_2^0$ decay, $m_{\tilde{\chi}_2^0}$, $m_{\tilde{\chi}_1^0}$ and $m_{\tilde{l}}$. The measurements are based on lepton distributions only and free from uncertainty due to jet energy smearing.

The organization of this paper is as follows. In Sec. II, we analyze the MSUGRA points which were studied in [2,8], where squark and gluino decays are the dominant sources of $\tilde{\chi}_2^0$. We concentrate on the case where $\tilde{\chi}_2^0 \to \tilde{l} l$ is open and followed by $\tilde{l} \to l \tilde{\chi}_1^0$. We find that the A_T distribution has a peak if $m_{ll} \lesssim m_{ll}^{\max}/2$ is required. In the limit where $m_{ll} \sim 0$, the peak *necessarily* agrees with the ratio of lepton energies $A_E^0 = E_{l2}/E_{l1}$ in the $\tilde{\chi}_2^0$ rest frame for any value of the $\tilde{\chi}_2^0$

velocity. A_E^0 is a simple function of the gaugino and slepton masses. We show that a small m_{ll} cut promises smaller systematic errors by comparing distributions for different neutralino velocities. In Sec. III, we show Monte Carlo (MC) simulations for the MSUGRA points. We find nearly perfect *quantitative* agreement between the expectation and MC data for wide parameter regions. In Sec. IV, we show that systematics due to the $\tilde{\chi}_2^0$ velocity distribution could be corrected by the hardest lepton's P_T distribution. We also show expected errors on gaugino and slepton masses. For the most optimistic cases where the end point of the lepton invariant mass distribution of the three body decay $m_{ll}^{3\,\mathrm{body}}$ is observed in addition to the edge of the m_{ll} distribution of the two body decay $m_{ll}^{2\,\mathrm{body}}$, we can determine $m_{\tilde{\chi}_2^0}$, $m_{\tilde{\chi}_1^0}$ and $m_{\tilde{l}}$ from this (almost) purely kinematical information. At least two degrees of freedom of the three mass parameters would be determined by our method if $m_{ll}^{\max} \gg 25$ GeV. Section V is devoted to discussions.

II. DISTRIBUTION OF LEPTON ENERGY ASYMMETRY WITH m_{ll} CUT

At hadron colliders, the second lightest neutralino $\tilde{\chi}_2^0$ would be produced in $\tilde{q}$ and $\tilde{g}$ decays, or in $\tilde{\chi}_1^\pm \tilde{\chi}_2^0$ pair production. The decay $\tilde{\chi}_2^0 \to \tilde{l} l$ could be a dominant decay mode if it is open. Followed by $\tilde{l} \to l \tilde{\chi}_1^0$, the signal consists of the same flavor and opposite sign lepton pair associated with some missing momentum. It is one of the most promising SUSY signals at hadron colliders.

The decay process $\tilde{\chi}_2^0 \to \tilde{l}^\pm l_1^\mp \to \tilde{\chi}_1^0 l_1^\pm l_2^\mp$ is described by two body kinematics and is very simple. The m_{ll} distribution of the lepton pair from the $\tilde{\chi}_2^0$ cascade decay is

$$\frac{1}{\Gamma}\frac{d\Gamma}{dm_{ll}^2} = \frac{1}{(m_{ll}^{\max})^2}, \tag{1}$$

where

$$m_{ll}^{\max} = \frac{\sqrt{(m_{\tilde{\chi}_2^0}^2 - m_{\tilde{l}}^2)(m_{\tilde{l}}^2 - m_{\tilde{\chi}_1^0}^2)}}{m_{\tilde{l}}}. \tag{2}$$

The decay distribution is flat in m_{ll}^2. The only physical information we can get from the m_{ll} distribution is therefore the value of the end point. It constrains one combination of the three masses involved in $\tilde{\chi}_2^0$ decay, as one can see in Eq. (2).

In the rest frame of the second lightest neutralino, the energy of l_1 is a function of $m_{\tilde{\chi}_2^0}$ and $m_{\tilde{l}}$, while E_{l_2} also depends on m_{ll} and $m_{\tilde{\chi}_1^0}$:

$$E_{l_1} = \frac{m_{\tilde{\chi}_2^0}^2 - m_{\tilde{l}}^2}{2m_{\tilde{\chi}_2^0}}, \quad E_{l_2} = \frac{m_{ll}^2 + m_{\tilde{l}}^2 - m_{\tilde{\chi}_1^0}^2}{2m_{\tilde{\chi}_2^0}}. \tag{3}$$

The angle θ_{ll} between the two leptons in the $\tilde{\chi}_2^0$ rest frame is obtained by solving

$$m_{ll}^2 = 2E_{l_1}E_{l_2}(1-\cos\theta_{ll}), \tag{4}$$

where $\theta = 0$ for $m_{ll} = 0$, while $\theta = \pi$ for $m_{ll} = m_{ll}^{\max}$.

In Eq. (3), we see that E_{l_1} is monochromatic in the $\tilde{\chi}_2^0$ rest frame. As a result, the energies of the two leptons are asymmetric. The ratio of the transverse momenta of the leptons, which we call the transverse momentum asymmetry $A_T = P_{T2}^l / P_{T1}^l$ $(P_{T1}^l > P_{T2}^l)$ provides more information on the decay kinematics.[1] However, P_{T1}^l and P_{T2}^l depend on the parent neutralino momentum, unlike the Lorentz invariant quantity m_{ll}. The $\tilde{\chi}_2^0$ velocity distribution in turn depends on $m_{\tilde{q}}$ and $m_{\tilde{g}}$, although the $\tilde{\chi}_2^0$ decay distribution in the $\tilde{\chi}_2^0$ rest frame itself does not depend on them.

This distribution has been used in global fits of MSUGRA parameters; A_T distribution ''data'' for one MSUGRA point generated by the MC simulator are compared to those of different MSUGRA points [5,8]. In this model, all sparticle masses depend on a few universal soft breaking parameters such as m_0, M, $\tan\beta$, etc. When we compare different MSUGRA points, we therefore change both the parameters of the $\tilde{\chi}_2^0$ decay, $m_{\tilde{\chi}_2^0}$, $m_{\tilde{\chi}_1^0}$ and $m_{\tilde{l}}$, and the parameters of $\tilde{\chi}_2^0$ momentum distributions $m_{\tilde{q}}$ and $m_{\tilde{g}}$ at the same time. Therefore it was considered to be less important compared to invariant mass distributions.

However it is possible to make a more direct connection with the first set of mass parameters $m_{\tilde{\chi}_2^0}$, $m_{\tilde{\chi}_1^0}$ and $m_{\tilde{l}}$ if a moderate m_{ll} cut is applied [9]. When m_{ll} is small compared to $m_{ll}^{\max}$, the lepton and antilepton nearly go in the same direction. Then the lepton momentum asymmetry becomes less sensitive to the parent neutralino velocity. Even after the smearing due to the boost of $\tilde{\chi}_2^0$, the value $A_E^0 \equiv E_1/E_2|_{m_{ll}=0}$ can still be extracted from the peak of $A_T = P_{T2}^l / P_{T1}^l$:

$$A_T^{\mathrm{peak}} (\mathrm{or}\ \ 1/A_T^{\mathrm{peak}}) \simeq A_E^0 \equiv \frac{m_{\tilde{\chi}_2^0}^2 - m_{\tilde{l}}^2}{m_{\tilde{l}}^2 - m_{\tilde{\chi}_1^0}^2}, \tag{5}$$

therefore A_T^{peak} constrains the mass parameters involved in $\tilde{\chi}_2^0$ deca, just as $m_{ll}^{\max}$ does. Note A_E^0 has monotonous dependence on all parameters while the m_{ll} edge might be accidentally insensitive on $m_{\tilde{l}}$.[2] Note also that the lepton from the $\tilde{\chi}_2^0$ and $\tilde{l}$ decays cannot be distinguished in the experiment. A_T is defined so that it is always less than 1, and it is understood that A_T^{peak} means $1/A_T^{\mathrm{peak}}$ when A_E^0 exceeds one in Eq. (5).

---

[1] One may also use the lepton energy ratio E_{l1}/E_{l2}. In general, P_T distribution reflects sparticle masses much better than energy distribution.

[2] We thank M. Drees for pointing this out.

TABLE I. Mass parameters and relevant sparticle masses in GeV for the points studied in this paper. ISAJET [10] is used to generate sparticle masses. We also show corresponding $m_{ll}^{\max}$ and A_E^0 in the table.

	IK	P5	P5-2	P5-1	P5-3
m(GeV)	100	100	115	120	125
M(GeV)	150	300	300	300	300
A(GeV)	0	300	300	300	300
$\tan\beta$	2	2.1	2.1	2.1	2.1
sgn(μ)	−	+	+	+	+
$m_{\tilde{e}_R}$(GeV)	120.7	157.2	167.1	170.6	174.2
$m_{\tilde{\chi}_1^0}$(GeV)	65.2	121.5	121.6	121.6	121.6
$m_{\tilde{\chi}_2^0}$(GeV)	135.4	233.0	233.2	233.3	233.3
$m_{ll}^{\max}$(GeV)	51.8	109.1	111.6	111.6	111.1
A_E^0	0.368	0.336	0.496	0.565	0.646

In this paper, we study the power of the A_T distribution in the low m_{ll} region ($m_{ll}<m_{ll}^{\max}/2$) to constrain the kinematics of the cascade decay $\tilde{\chi}_2^0\to\tilde{l}l\to\tilde{\chi}_1^0 ll$. We chose the points shown in Table I, but our method can be applied in generic MSSM studies. Unlike the common approach to immediately go into full MC simulations, we first study the decay distribution for fixed neutralino velocity (labeled by the boost factor $\gamma_{\tilde{\chi}_2^0}$ and the pseudorapidity $\eta_{\tilde{\chi}_2^0}$) $\Gamma(A_T(\gamma_{\tilde{\chi}_2^0},\eta_{\tilde{\chi}_2^0}))$.[3]

The distribution we observe in experiments is expressed by convoluting the distribution with the velocity distribution of $\tilde{\chi}_2^0$, $F(\gamma,\eta)$, as follows:

$$d\sigma(A_T)\equiv\int d\gamma d\eta F(\gamma,\eta)\Gamma(A_T(\gamma,\eta)) \qquad (6)$$

the measured distribution is also affected by cuts on $\not{E}_T$, $M_{\rm eff}$, etc. However it is still useful to know how $\Gamma(A_T(\gamma_{\tilde{\chi}_2^0},\eta_{\tilde{\chi}_2^0}))$ depends on the underlying mass parameters and the $\tilde{\chi}_2^0$ velocity.

In Fig. 1, we show the A_T distribution with/without invariant mass cuts and P_T^l cuts. Here we take the IK point and $\gamma_{\tilde{\chi}_2^0}=1.9$, $\eta_{\tilde{\chi}_2^0}=0.2$. The distribution is easily obtained by numerical integration.

The distribution without upper m_{ll} cut has some structure around $A_T=0.3$ (top solid histogram), but it is insignificant. (Here we took the events with $m_{ll}>12$ GeV because large backgrounds from virtual photons are expected for $m_{ll}<12$ GeV [11].) With the cut $P_T^l>10$ GeV and the same $\tilde{\chi}_2^0$ velocity, events with $A_T<0.1$ are hardly accepted, and the distribution is roughly flat between $0.2<A_T<0.3$ (top dashed histogram). When the lepton energy in the $\tilde{\chi}_2^0$ rest frame is small, the acceptance efficiency of the events strongly depends on the velocity of $\tilde{\chi}_2^0$, because of the P_T^l cut. The A_T distribution would depend on the cuts and the distribution of $\tilde{\chi}_2^0$ velocity introducing systematical errors to the analysis.

On the other hand, once a moderate m_{ll} cut is applied, the decay distribution becomes nearly independent of P_T^l cuts (bottom histograms). Here we integrate the region between 12 GeV$<m_{ll}<$25 GeV$\sim m_{ll}^{\max}/2$. The distribution has a peak at $A_T\sim A_E^0=0.368$. The peak is outside the small A_T region affected by the P_T^l cut. It is also clear from the plot that the shoulder of the distribution without m_{ll} cut comes from the events with $m_{ll}<25$ GeV. Note that $\cos\theta_{ll}=0.86(0.44)$ for $m_{ll}=12(25)$ GeV in the $\tilde{\chi}_2^0$ rest frame,

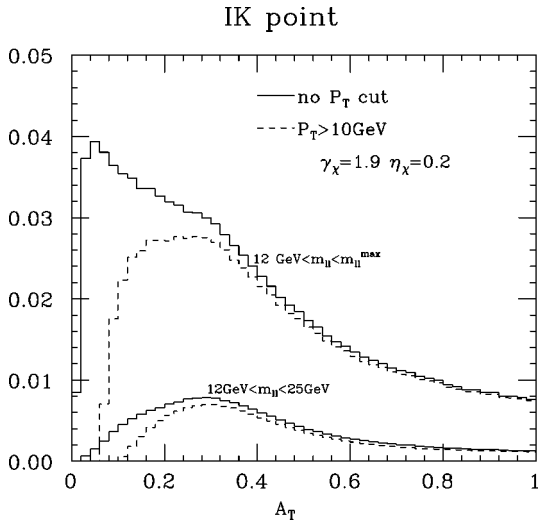

FIG. 1. A_T distribution for the $\tilde{\chi}_2^0$ momentum $(\gamma_{\tilde{\chi}_2^0},\eta_{\tilde{\chi}_2^0})=(1.9, 0.2)$ without P_T^l cut (solid), and for $P_T^l>10$ GeV (dashed). Overall normalization is arbitrary. The upper histograms are without upper m_{ll} cut while the lower histograms are distributions with $m_{ll}<25$ GeV.

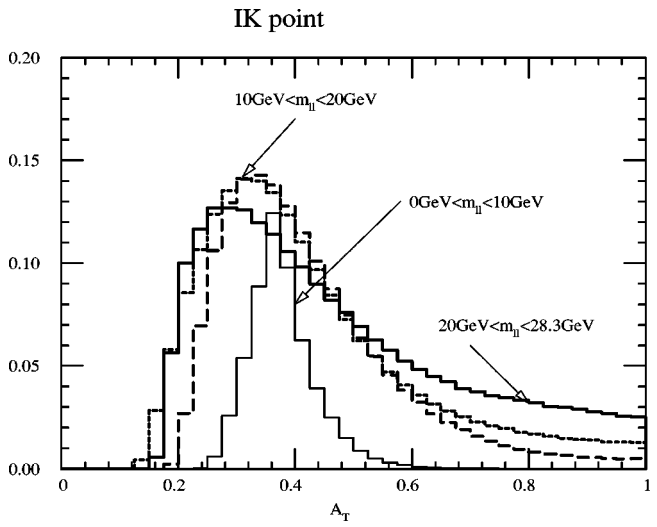

FIG. 2. A_T distribution under different m_{ll} cuts. $(\gamma_{\tilde{\chi}_2^0},\eta_{\tilde{\chi}_2^0})=(1.4, 0.2)$, and $P_T^l>10$ GeV for solid and dashed histogram, while the dotted histogram is for $\gamma_{\tilde{\chi}_2^0}=2.3$ and $\eta_{\tilde{\chi}_2^0}=0.2$. Overall normalization is arbitrary.

[3]The decay distribution Γ depends on γ and η through the Lorentz boost of all momenta, which is implicitly shown as $A_T(\gamma,\eta)$, or $P_T^l(\gamma,\eta)$.

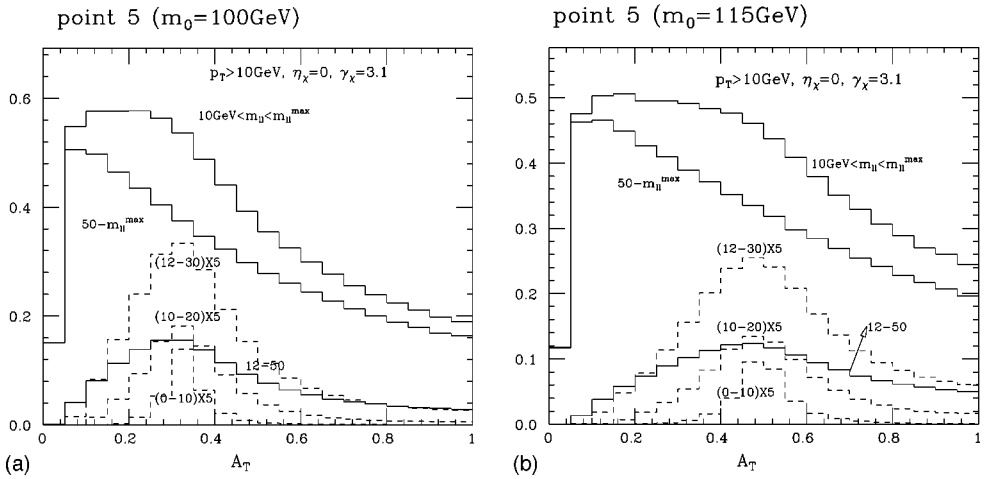

FIG. 3. A_T distributions for different invariant mass cuts. $\gamma_{\tilde{\chi}_2^0}=3.1$, $\beta_{\tilde{\chi}_2^0}=0$. The distribution for tight m_{ll} cuts are scaled by a factor of 5.

therefore the angle between the lepton and the antilepton in the pair is rather small with the m_{ll} cut.

To put it differently, events above $m_{ll}^{\max}/2$ are merely *backgrounds* to the A_E^0 measurement. This is easily understood when we consider the lepton configuration near the m_{ll} end point. The two leptons go in exactly opposite directions and the asymmetry is modified maximally when one of the leptons goes in the direction of $\tilde{\chi}_2^0$ momentum, $A \equiv E_1^{\rm lab}/E_2^{\rm lab}=A_E|_{m_{ll}=m_{ll}^{\max}}\times(1\pm\beta)/(1\mp\beta)$, where $A_E=0.29$ and $\beta=0.855$ for Fig. 1. The lepton energy asymmetry in the laboratory frame can range from nearly 0 to 1 due to the boost.

It is worth noting that the A_T distribution peaks at a smaller value of A_T as one increases the m_{ll} cut. In Fig. 2, we show distributions with different m_{ll} cuts, 0 GeV$<m_{ll}<$10 GeV (solid thin), 10 GeV$<m_{ll}<$20 GeV (dashed), 20 GeV$<m_{ll}<$28.3 GeV (solid thick), for $\gamma_{\tilde{\chi}_2^0}=1.4$ and $\eta_{\tilde{\chi}_2^0}=0.2$. The distribution has a sharp peak at a position consistent with A_E^0 for the sample with $m_{ll}<10$ GeV. $A_T^{\rm peak}=0.323$ for the same neutralino velocity for 10 GeV $<m_{ll}<20$ GeV (dashed histogram). This shift cannot be explained by A_E deviation from $A_E^0(A_E=0.363(0.354))$ for $m_{ll}=10(20)$ GeV, but it comes from the smearing of A_T distribution for the finite lepton angle.

The dotted histogram shows a distribution for a higher neutralino velocity $\gamma=2.3$ and $\eta=0.2$ with 10 GeV$<m_{ll}<$20 GeV. The peak position is shifted very little, $A_T^{\rm peak}\sim0.321$, therefore it may still be used to determine the decay kinematics.[4] On the other hand, the distribution off the peak depends more on the neutralino velocity. Using the whole distribution introduces a dependence on the $\tilde{\chi}_2^0$ momentum distribution, and the fit would be more assumption dependent.

The distribution is more and more smeared out and peaks at a lower A_T for larger m_{ll} cuts. The dependence on the $\tilde{\chi}_2^0$ momentum is also bigger for the large m_{ll} sample; $A_T^{\rm peak}=0.26(0.24)$ for $\gamma=1.4(2.3)$ and 20 GeV$<m_{ll}<$28.3 GeV. (Only the distribution for the former is shown in the figure.) The distribution is shifted to smaller A_T reducing the acceptance of the $P_T^l>10$ GeV cut. Some information on the neutralino velocity distribution is therefore necessary to deduce the neutralino decay kinematics from the A_T distribution while increasing the m_{ll} cut in order to increase the statistics and remove virtual photon backgrounds. This will be discussed in detail in Sec. IV.

Note that $m_{ll}^{\max}\sim50$ GeV for IK, therefore requiring $m_{ll}<25$ GeV reduces the number of events in the sample by 1/4. The reward is a distribution which is less sensitive to P_T^l cuts and to the $\tilde{\chi}_2^0$ velocity distribution, and a simple correspondence to the quantity in the $\tilde{\chi}_2^0$ rest frame.

Finally we demonstrate sensitivity of the A_T distribution to the slepton mass. We first compare distributions with different slepton masses, P5 ($m_0=100$ GeV) and P5-2 ($m_0=115$ GeV) in Figs. 3(a) and 3(b). Here we try a relatively large $\gamma_{\tilde{\chi}_2^0}$ in order to have a substantial effect from the $\tilde{\chi}_2^0$ boost ($\gamma=3.1$ $\eta=0$). Still, the distributions are clearly peaked at $A_T\sim0.32$ (P5) 0.48 (P5-2) for events with $m_{ll}<50$ GeV, while the distribution with $m_{ll}>50$ GeV does not show any structure between $A_T=0.1$–1. Note $m_{ll}=50$ GeV roughly corresponds to half of $m_{ll}^{\max}$ again.

In Fig. 4, we compare distributions with different m_0. Peak positions shift from 0.3 to 0.63 as one changes m_0 by 25 GeV. If systematic errors are negligible and M is fixed, the sensitivity to m_0 would be $\delta m_0\sim1.6$ GeV for $\delta A=0.02$ (as will be found in Sec. III). The peaks are consistent with $A_E^0=0.33$ (for $m_0=100$ GeV), 0.49 (for $m_0=115$ GeV) and 0.65 (for $m_0=125$ GeV). In Sec. III, we will find similar agreement for full MC simulation data, establishing the correspondence.

[4]Peaks are determined by fitting the distribution near the peak to a polynomial fitting function.

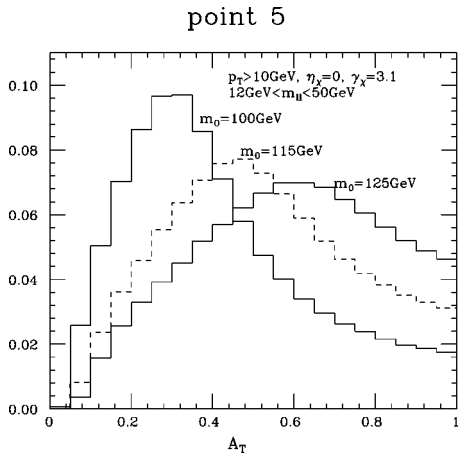

FIG. 4. A_T distributions for different slepton masses. Cuts are 12 GeV$<m_{ll}<$50 GeV, $P_T^l>10$ GeV. $(\gamma,\eta)=(3.1,0)$.

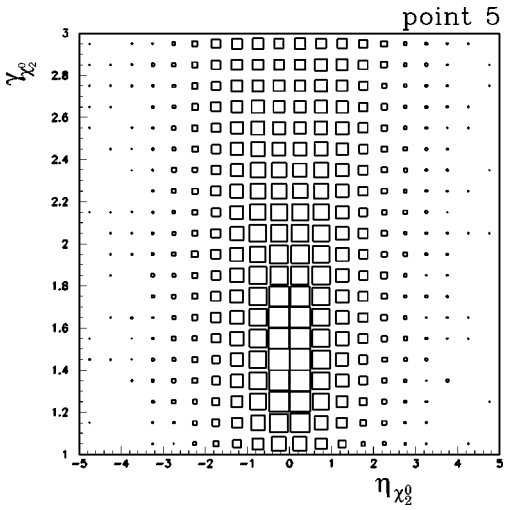

FIG. 5. (η,γ) distribution of $\tilde{\chi}_2^0$ for point 5.

III. MONTE CARLO SIMULATIONS

We are now ready to perform full MC simulations to check the observations made in Sec. II.

We use ISAJET 7.42 [10] to generate SUSY events. The generated events are analyzed by the simple detector simulator ATLFAST2.21 [12]. The cuts to remove the SM backgrounds down to a negligible level have already been studied in [5,8]; they are summarized as follows.

A. IK (inclusive three lepton channel) [8]

For this point, $M_{\rm eff}$ and $\not{E}_T$ cuts are not efficient because of the light $\tilde{g}$. A third tagging lepton from $\tilde{\chi}_2^0$ or $\tilde{\chi}_1^+$ decay is required. When three leptons are in the same flavor, the pair of leptons with smaller ΔR is selected as a lepton pair candidate.

(i) Two opposite sign same flavor leptons with $P_T^l>15$ GeV;

(ii) Third tagging lepton with $P_T^l>15$ GeV;

(iii) Lepton isolation; No $P_T>2$ GeV track within a $\Delta R<0.3$ cone centered on the lepton track; and

(iv) $\not{E}_T>200$ GeV.

B. Point 5 [5]

(i) four jets with $P_{T1}>100$ GeV and $P_{T2,3,4}>50$ GeV;

(ii) $M_{\rm eff}\equiv P_{T,1}+P_{T,2}+P_{T,3}+P_{T,4}+\not{E}_T>400$ GeV;

(iii) $\not{E}_T>\max(100\ {\rm GeV}, 0.2M_{\rm eff})$; and

(iv) Two isolated leptons with $P_T^l>10$ GeV, $|\eta|<2.5$.

Isolation is defined as less than 10 GeV energy deposit within a $\Delta R<0.2$ cone centered on the lepton track.

We generate 2×10^6 events for each point. This roughly corresponds to 5 fb^{-1} for IK, and 100 fb^{-1} for point 5. We present distributions without cuts on $M_{\rm eff}$, jet P_T and $\not{E}_T$. In previous simulations [5,7,8], the acceptance is roughly constant for all values of m_{ll}, therefore those cuts are expected not to modify the lepton distributions substantially. Note that substantial acceptance for events with $m_{ll}<m_{ll}^{\rm max}/2$ is crucial for using the information from the A_T distribution, as we have seen in Sec. II.

We keep some lepton isolation cuts: less than 10 GeV energy deposit within a $\Delta R<0.2$ (0.3 for IK) cone centered on the lepton track; no jet within a $\Delta R<0.4$ cone centered on a lepton track.[5]

Note that we do not follow the isolation cut given in IK [8], again because they do not affect the signal distribution.

The acceptance of events turns out to be too high by a factor of 3(2.5) for point 5(IK) compared to a full analysis including the jet related cuts [8,5,7]. This factor is taken into account when we interpret the fitting results.[6] No plot or fit in this section contains SM background, while SUSY background is included.

In the previous section, we have already seen that the A_T distribution is somewhat dependent on the parent neutralino velocity $(\gamma_{\tilde{\chi}_2^0}, \eta_{\tilde{\chi}_2^0})$. In Fig. 5, we show the $\gamma_{\tilde{\chi}_2^0}$ and $\eta_{\tilde{\chi}_2^0}$ distribution for point IK. Here one can see that $\eta_{\tilde{\chi}_2^0}$ is roughly within $|\eta|\lesssim1$. The $\tilde{\chi}_2^0$ can be very relativistic; $\gamma_{\tilde{\chi}_2^0}$ could be much larger than 2. A modification of the A_T distribution due to Lorentz boosts is expected unless some m_{ll} cut is applied. The P_T^l distribution is shown in Fig. 6. Here we plot the distribution of the higher (lower) of two lepton P_T for the dotted (solid) line. The first (higher) lepton P_T^l can be a few times higher than its most probable value, reflecting the existence of relativistic $\tilde{\chi}_2^0$ in the signal sample.

We now study the asymmetry distribution in Fig. 7. The plot for point IK [Fig. 7(a)] shows a smeared peak at $A_T\sim0.36$, but the peak is rather flat at the top. For point 5 [Fig.

[5]We use the jet finding algorithm of ATLFAST. The jet cone size is $\Delta R_j<0.4$. The jet finding algorithm requires 1.5 GeV of minimum energy deposit for the cluster seed, jet cone size $\Delta R_j<0.4$, 10 GeV minimum total energy. A resulting cluster with energy more than 15 GeV is called jet.

[6]The number of the selected events for the IK point is 7000 between 10 GeV to 20 GeV even for the small integrated luminosity of 5 fb^{-1} [8]. Therefore, the systematic errors would be dominant for this point.

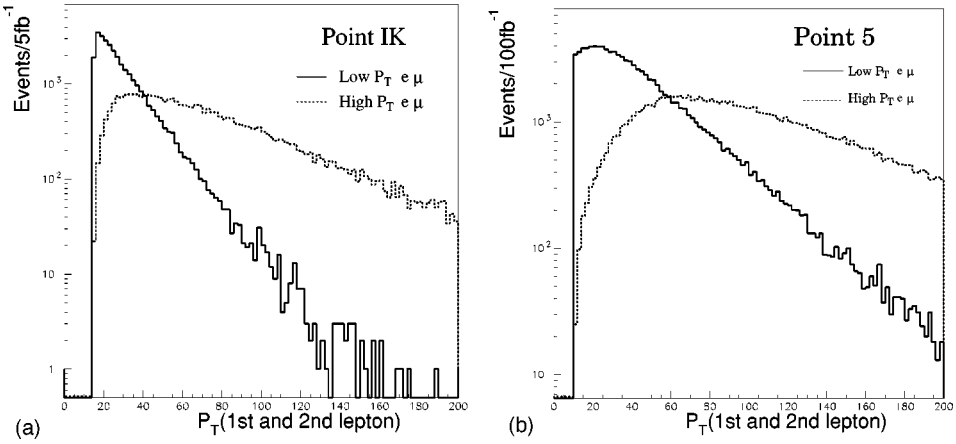

FIG. 6. Lepton P_T distributions of the first (high) and the second (low) P_T leptons for: (a) IK and (b) point 5.

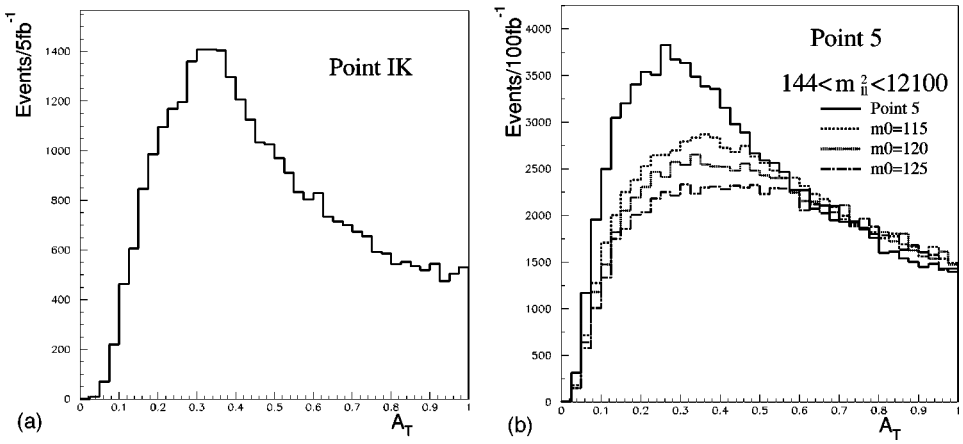

FIG. 7. A_T distribution for: (a) IK and (b) point 5 without upper m_{ll} cut.

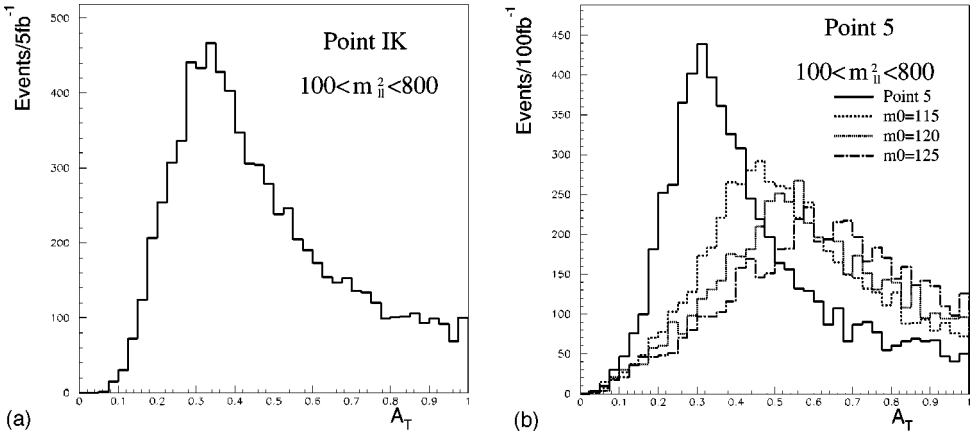

FIG. 8. A_T distribution with a 100 $(\mathrm{GeV})^2 < m_{ll}^2 < 800$ $(\mathrm{GeV})^2$ cut.

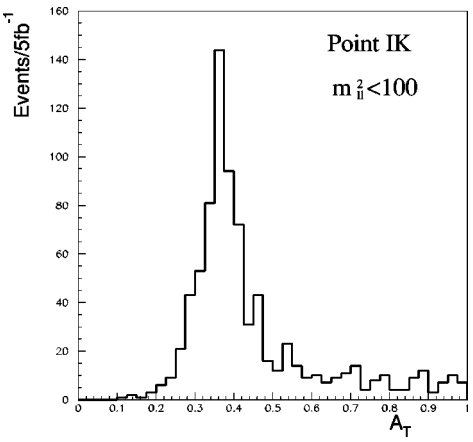

FIG. 9. A_T distribution for point IK: $m_{ll}<10$ GeV.

7(b)], the distribution has even less structure, especially when $m_0>115$ GeV. Although global fits of the distributions must give us information on the neutralino decay kinematics, the power to constrain neutralino decay parameters would be limited if we try to analyze models without the constraint between soft breaking parameters.

In Fig. 8, we show A_T distributions with m_{ll} cut, 100 $(\mathrm{GeV})^2<m_{ll}^2<800$ $(\mathrm{GeV})^2$. We find a narrower peak for point IK compared to the case without invariant mass cut. For point 5, improvement of the signal distribution compared to Fig. 7 is clear. The peak position moves right as m_0 is increased, and it is consistent with Fig. 4. Note that for point 5 (IK), $m_{ll}^2<800$ $(\mathrm{GeV})^2$ corresponds to $\cos\theta_{ll}=0.72(0.29)$. The angle between the two leptons is smaller for point 5, which explains the substantial improvement for point 5.

In Fig. 9, we show the distribution of the events with $m_{ll}<10$ GeV for point IK. The peak is now nearly δ function like, and it agrees with A_E^0. Unfortunately, one would not be able to use this information to measure A_E^0 directly. There could be a significant background for the events below $m_{ll}<12$ GeV as recently discussed in [11]. (See discussion in Sec. IV for details.)

We now fit the MC data to a phenomenological fitting function to determine the peak positions and the associated errors. The fitting function is chosen as follows:

$$N(A)=N_0\exp\left(-0.5\times\left(\frac{A-A_0}{\sigma}\right)^2\right) \quad \text{for } A<A_0,$$
$$N(A)=N_0\ \exp(-f(A-A_0)) \quad \text{for } A>A_0, \tag{7}$$

where parameters A_0, f, N_0, and σ are determined by minimizing χ^2 using the program MINUIT.[7]

Results of these fits are shown in Fig. 10. For IK [Fig. 10(a)] we fit the A_T distribution of events with 10 GeV $<m_{ll}<14.14$ GeV and find $A_0=0.3408\pm0.01$. This number is obtained based on the MC data corresponding to only 5 fb^{-1} of the integrated luminosity, although we do not impose the same cuts with IK. As we noted earlier, if cuts are the same as those of [8], the total number of events would be reduced by a factor of 2.5, but that would be easily compensated by the accumulation of luminosities.

The peak position is smaller than $A_E^0=0.36$ [defined in Eq. (5)]. However, the A_T distribution for fixed neutralino velocity $(\gamma,\eta)=(1.4,0.2)$ indeed peaks at 0.34 if 10 GeV $<m_{ll}<14.14$ GeV, consistent with the full MC simulation. It is not clear if such a low m_{ll} region can be used for the fit due to the large background expected in this region. (See Sec. IV in detail.) However, the reproduction of the simple estimations in Sec. II is still impressive. As discussed earlier, the peak position does not depend strongly on neutralino velocity when a tight m_{ll} cut is imposed. The m_{ll} cut would be beneficial provided there are enough statistics and manageable background.

For point 5 [Figs. 10(b)–10(d)], we use the events for 10 GeV$<m_{ll}<28.3$ GeV for the fit: $A_0=0.324\pm0.005$, 0.491 ± 0.012, and 0.675 ± 0.018 for $m_0=100$, 115 and 125 GeV, respectively. The m_{ll} cut dependence is rather small; A_E^0 is 0.33, 0.49, and 0.65 respectively, already consistent with the fit.[8] Recall again that our simulation does not include jet related cuts. The total number of events is a factor of 3 too large for those with the full cut. The error under the full cut for 100 fb^{-1} integrated luminosity is 0.009, 0.02, and 0.03 for points 5, 5-2, and 5-4, respectively, assuming statistical scaling.

IV. MODEL INDEPENDENT MASS DETERMINATION

The second lightest neutralino might arise from squark and gluino decays at hadron colliders, therefore the $\tilde{\chi}_2^0$ velocity distribution should depend on $m_{\tilde{q}}$ and $m_{\tilde{g}}$. One may, in principle, fit the whole distribution to determine model parameters completely, but various systematic errors could prevent a complete understanding of the event structure. We wish to stay with the distribution which is less model dependent and free of systematics. Invariant mass distributions are a well established candidate for such a distribution. In the previous sections we argued that the peak position of the A_T distribution can be almost independent of the $\tilde{\chi}_2^0$ velocity distribution if certain cuts are applied on m_{ll}.

In this section, we will find that the remaining minor $\gamma_{\tilde{\chi}_2^0}$, $\eta_{\tilde{\chi}_2^0}$ distribution dependence may be removed by looking into the first lepton P_T distribution. In Fig. 11(a), we show the A_T distributions for different $\tilde{\chi}_2^0$ velocity. We took point IK and 12 GeV$<m_{ll}<25$ GeV, therefore the distribution is somewhat dependent on the neutralino velocity, especially when $\gamma_{\tilde{\chi}_2^0}$ is small. A_T^{peak} shifts from 0.31 to 0.29 between the rep-

[7]Here we take a completely phenomenological assumption for the fitting function, however it is much better to use the fitting function based on the neutralino velocity distribution calibrated by the first lepton P_T^l distribution. See Sec. IV.

[8]Note that the peak positions are at larger A_T compared to Fig. 4. This is because we select the events below $m_{ll}<28.3$ GeV for Fig. 8, while it is $m_{ll}<50$ GeV in Fig. 4.

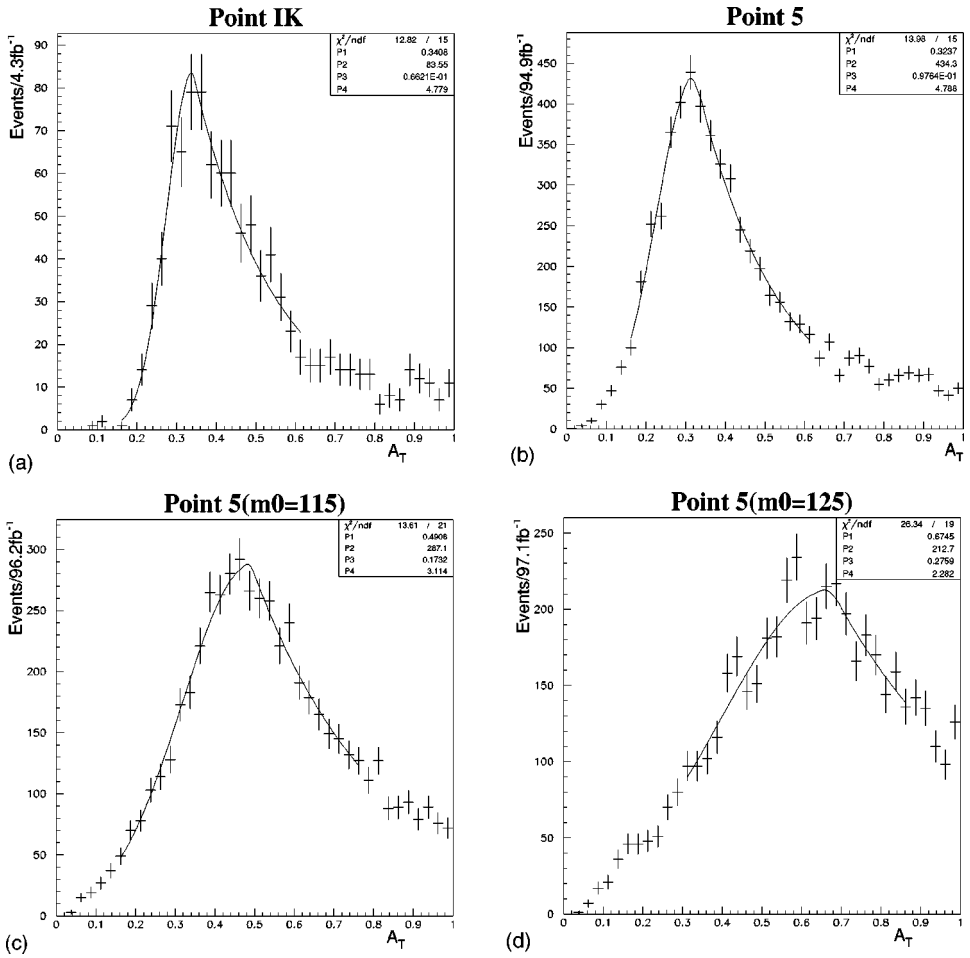

FIG. 10. Fits to the MC data using the fitting function 7: (a) IK, (b) point 5, (c) point 5-2, and (d) point 5-4.

resentative neutralino velocity. In the same figure we also show distributions for $m_{\tilde{l}}=117.68$ GeV. In this case the peak moves from 0.42 to 0.37. The velocity dependence is slightly stronger than for the IK point. Although the peak position itself does not depend too much on the velocity, this certainly suggests some systematics would come into the fit to the decay parameters.

The $\tilde{\chi}_2^0$ velocity distribution strongly affects the hardest lepton P_T distribution, as one can see in Fig. 11(b). Here the three distributions corresponding to Fig. 11(a) have totally different P_T^l end points. We can imagine that the systematics coming from the neutralino velocity dependence would be substantially reduced if the P_T^l distribution is included in the

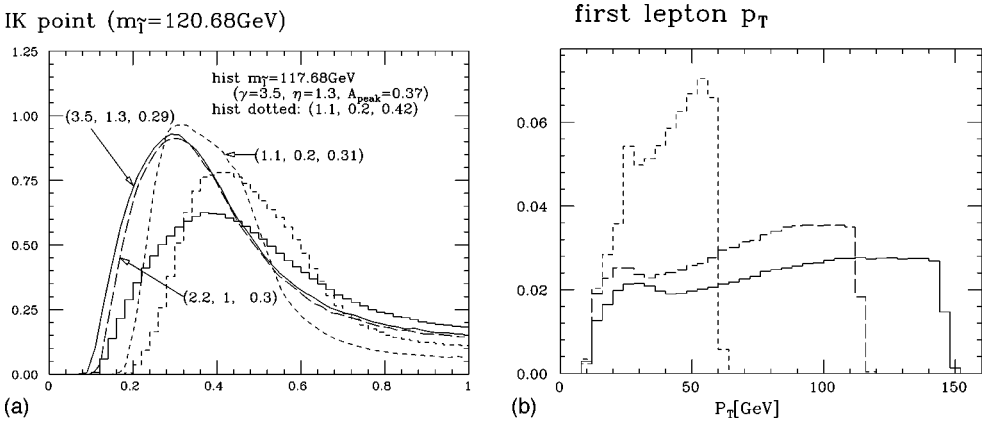

FIG. 11. (a) A_T and (b) P_T^l distributions for different $\tilde{\chi}_2^0$ velocity $(\gamma,\eta)=(1.1,0.2)$, (2.2,1), and (3.5,1.3). $A_T^{\rm peak}$ of each distribution is also indicated in the figure. We also show the histogram for $m_{\tilde{l}}=117.68$ GeV in (a) for comparison.

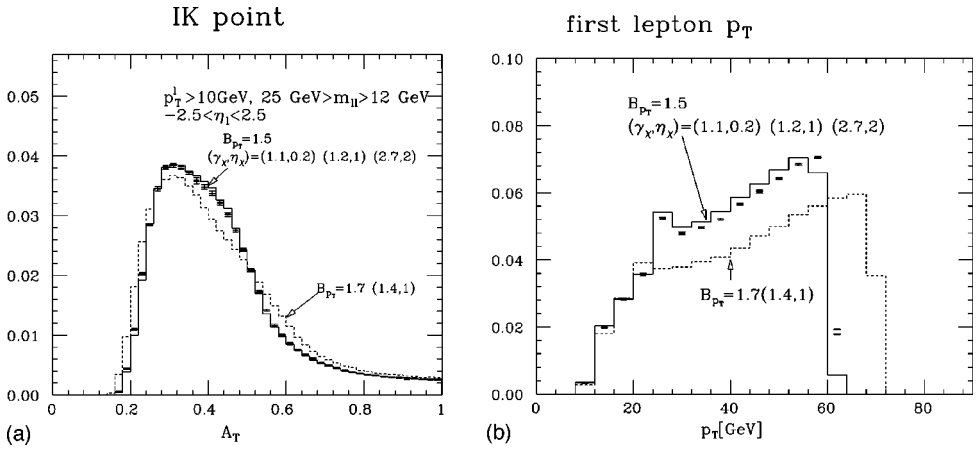

FIG. 12. A_T and P_T^l distributions for different neutralino velocities but the same transverse boost factor B_T. Solid histogram is for $(\gamma,\eta)=(1.1,0.2)$ while bar graphs are for $(\gamma,\eta)=(1.2,1)$ and $(2.7,2)$. Errors of numerical integrations are shown as bar size. Two bars in the same bin almost coincide. A distribution with a different transverse boost factor is shown by the dotted histogram.

fit as well.

The A_T and P_T^l distributions can be expressed as convolutions of the neutralino velocity distribution and neutralino decay distributions as follows:

$$\sigma(A_T)=\int d\gamma_{\tilde{\chi}_2^0} d\eta_{\tilde{\chi}_2^0} F(\gamma_{\tilde{\chi}_2^0},\eta_{\tilde{\chi}_2^0})\times\Gamma(A_T(\gamma_{\tilde{\chi}_2^0},\eta_{\tilde{\chi}_2^0})), \tag{8}$$

$$\sigma(P_T^l)=\int d\gamma_{\tilde{\chi}_2^0} d\eta_{\tilde{\chi}_2^0} F(\gamma_{\tilde{\chi}_2^0},\eta_{\tilde{\chi}_2^0})\times\Gamma(P_T^l(\gamma_{\tilde{\chi}_2^0},\eta_{\tilde{\chi}_2^0})). \tag{9}$$

The neutralino velocity distribution $F(\gamma,\eta)$ depends on parent sparticle masses, while the decay distributions in the laboratory frame $\Gamma(A_T)$ and $\Gamma(P_T^l)$ depend on $m_{\tilde{\chi}_1^0}$, $m_{\tilde{\chi}_2^0}$ and $m_{\tilde{l}}$ implicitly. Various cuts would be applied to experimental samples of events, therefore these equations are rather schematic. Note that the two distributions have a different neutralino velocity dependence. The $\eta_{\tilde{\chi}_2^0}$ and $\gamma_{\tilde{\chi}_2^0}$ dependence tend to cancel in $A_T(\gamma,\eta)$, while the transverse momentum in the laboratory frame $P_T^l(\gamma,\eta)$ keeps increasing with γ. Hence a measurement of the P_T^l distribution must be very useful for correcting the minor dependence of the A_T distribution on $\eta_{\tilde{\chi}_2^0}$ and $\gamma_{\tilde{\chi}_2^0}$.

The parent neutralino velocity can be decomposed into a boost γ_T from the $\tilde{\chi}_2^0$ rest frame transverse to the beam direction, followed by a boost γ_L in the beam direction. When we assume uniform neutralino decay, the A_T and P_T^l distributions depend on the γ_T distribution while the latter distribution has no effect on them. This can be seen in Figs. 12(a) and 12(b). We show three A_T and P_T^l distributions for $\tilde{\chi}_2^0$ $(\gamma_{\tilde{\chi}},\eta_{\tilde{\chi}})=(1.1,0.2)$, $(1.2,1)$ and $(2.7,2)$. The three points have a common feature

$$B_T(\gamma,\eta)\equiv\frac{P_T^l|_{\max}}{E_{l1}(\text{at}\,\tilde{\chi}_2^0\ \text{rest})}=1.5. \tag{10}$$

The P_T^l and A_T distributions of leptons are very similar as one can see in Figs. 12(a) and 12(b).

This observation is based on a numerical integration which now takes into account the cut $|\eta_l|<2.5$, in addition to 12 GeV $<m_{ll}<25$ GeV, and the $P_T^l>10$ GeV cut. The effect of the η_l cut turns out to be very small. We checked numerically that the distributions with common P_T^l end points are roughly the same with these cuts. On the other hand, the A_T distribution has significant B_T dependence as one can see from the distributions for $B_T=1.7$ (dotted histograms). This suggests that one only has to know the γ_T distribution, which could be reconstructed from the P_T^l distribution. Schematically, one can write

$$\sigma(A_T)=\int dB_T F(B_T)\times\Gamma(A_T(B_T(\eta,\gamma))), \tag{11}$$

$$\sigma(P_T^l)=\int dB_T F(B_T)\times\Gamma(P_T^l(B_T(\eta,\gamma))). \tag{12}$$

$\Gamma(A_T(B_T))$, and $\Gamma(P_T^l(B_T))$ are implicit functions of gaugino and slepton masses, and one can fit to experimental data to obtain those mass parameters in addition to $F(B_T)$. Of course, one must also study the effect of $\not{E}_T$, M_{eff}, and P_{Tj} cuts and detailed MC simulations are necessary.

Given the indication that the dependence on the $\tilde{\chi}_2^0$ velocity distribution can be corrected directly from the P_T^l distribution, we now use the error on A_T^{peak} and m_{ll} end points to determine $m_{\tilde{\chi}_2^0}$, $m_{\tilde{\chi}_1^0}$, and $m_{\tilde{l}}$. As we have seen in the previous sections, A_T^{peak} depends on the m_{ll} cut, but we assume the statistical uncertainty of A_T^{peak} can be translated into that of A_E^0; i.e., we assume that the correlation caused by only using events within a finite range of m_{ll} values would be small.

We take the IK point as an example; the point is interesting because both the edge of the m_{ll} distribution due to the two body cascade decays $m_{ll}^{2\,\text{body}}$ and the end point of the three body decay $\tilde{\chi}_2^0\to l l\tilde{\chi}_1^0$, $m_{ll}^{3\,\text{body}}$ can be seen. (See Fig. 13.) This is because the right handed slepton-lepton-wino (or

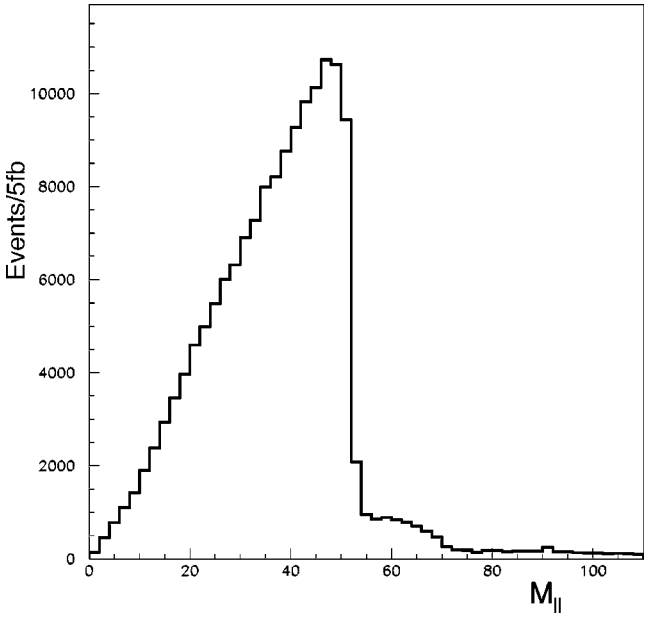

FIG. 13. The m_{ll} distribution for point IK.

Higgsino) coupling is (essentially) zero, therefore the two body decay coupling is suppressed. The measurements of $m_{ll}^{2\,\mathrm{body}}$, A_T^0, and $m_{ll}^{3\,\mathrm{body}} \equiv m_{\tilde{\chi}_2^0} - m_{\tilde{\chi}_1^0}$ are potentially sufficient to determine all sparticle masses involved in the $\tilde{\chi}_2^0$ cascade decay.

In order to demonstrate the importance of the measurement of A_T, we first show the expected constraints on $m_{\tilde{l}}$ and $m_{\tilde{\chi}_1^0}$ when $m_{\tilde{\chi}_2^0}$ is fixed. Note that the statistics could be $O(10)$ times larger than those given in Figs. 10(a) and 14, once $\int dt\mathcal{L} = 100\ \mathrm{fb}^{-1}$ is accumulated. It is expected that errors are dominated by the systematical ones for such high luminosity. We assume that A_T and $m_{ll}^{2\mathrm{body}}$ are measured within errors of 0.007 and 0.5 GeV, respectively (Fig. 14). $\Delta\chi^2$ is defined as

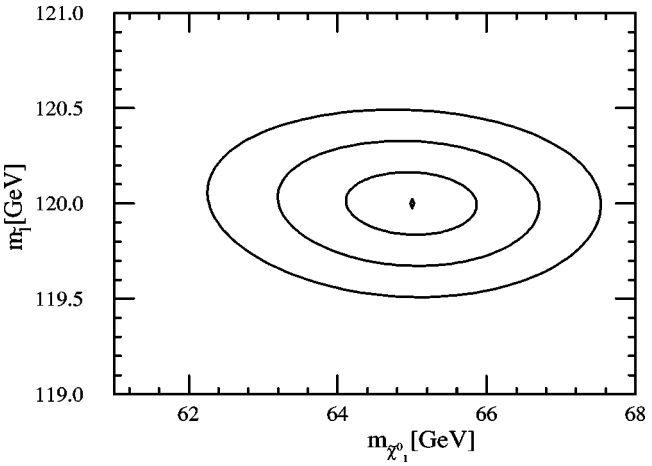

FIG. 14. Contours of constant $\Delta\chi^2 = 1,4,9$ for the IK point. We set $\delta m_{\tilde{\chi}_2^0} = 0$, $\delta m_{ll}^{2\ \mathrm{body}}$ 0.5 GeV, and $\delta A_E^0 = 0.007$. Only the contours near the input value are shown.

$$\Delta\chi^2 = \left(\frac{A_E^0 - A_E^{0\prime}}{\delta A_E^0}\right)^2 + \left(\frac{m_{ll} - m'_{ll}}{\delta m^{2\mathrm{body}}}\right)^2. \tag{13}$$

Here, A_E^0, δA_E^0 and $m_{ll} \equiv m_{ll}^{2\mathrm{body}}$ and $\delta m_{ll}^{2\mathrm{body}}$ are ''data'' and the error, while $A_E^{0\prime}$ and m'_{ll} are functions of the gaugino and slepton masses. The resulting $\Delta\chi^2 = 1,4,9,\ldots$ contours roughly correspond to $1\sigma, 2\sigma, 3\sigma, \ldots$ errors on the parameters. The errors on $m_{\tilde{l}}$ and $m_{\tilde{\chi}_1^0}$ could be on the order of 1% or less, consistent with the previous fits in [8]. Note, however, that they did not identify the origin of the peak structure and used the *whole* A_T distribution for the fit. As we have stressed, this fit will depend on assumptions about parent squark and gluino masses, while our fit relies solely on the peak position, directly constraining $m_{\tilde{\chi}_1^0}$, $m_{\tilde{\chi}_2^0}$ and $m_{\tilde{l}}$.

For the IK point, one can also determine $m_{ll}^{3\mathrm{body}}$. The errors on the masses under the three constraints would be substantially larger than those shown in Fig. 14 (where $m_{\tilde{\chi}_2^0}$ is fixed). This is due to correlations between the constraints. This can be seen in Fig. 15, where $m_{\tilde{\chi}_2^0}$ and $m_{\tilde{l}}$ are shown as functions of $m_{ll}^{3\,\mathrm{body}}$ for fixed values of A_E^0 and $m_{ll}^{2\mathrm{body}}$. Even in the limit where A_E^0 and $m_{ll}^{2\,\mathrm{body}}$ are known exactly, an error on $m_{ll}^{3\,\mathrm{body}}$ on the order of 1 GeV would result in 5 GeV errors on $m_{\tilde{\chi}_2^0}$ and $m_{\tilde{l}}$.

Assuming an error on $m_{ll}^{3\,\mathrm{body}}$, $\delta m_{ll}^{3\,\mathrm{body}} = 1$ GeV,[9] $m_{\tilde{\chi}_1^0}$, $m_{\tilde{\chi}_2^0}$, and $m_{\tilde{l}}$ are constrained within $\sim \pm 8$ GeV, without assuming any relation between gaugino and slepton masses. The error is large compared to those expected from LC experiments, however it still makes an impressive case where sparticle masses are determined without relying on model assumptions.[10]

Note that the $m_{\tilde{e}}/m_{\tilde{\mu}}$ ratio would be constrained strongly. Assuming $\delta A_T < 0.007$, $\delta m_{ee,\mu\mu} < 0.5$ GeV, $\delta m_{ll}^{3\,\mathrm{body}} = 4$ GeV, we obtain $\delta(m_{\tilde{e}}/m_{\tilde{\mu}}) = 2.5\%$ for $\Delta\chi^2 < 1$, and 7% for $\Delta\chi^2 < 9$.

Several comments are in order. The background in the region $m_{ll} \ll m_{ll}^{\max}$ must be studied carefully. For example, SM $t\bar{t}ll$ production could be important in the low m_{ll} region. The full amplitude study of $t\bar{t}ll$ or other production processes is necessary to determine the lower m_{ll} cut. Note that full amplitude level studies of $W\gamma^*$ production have been performed for the background process of $\tilde{\chi}_2^0\tilde{\chi}_1^\pm \to 3l$, and large background was found in the $m_{ll} < 10$ GeV region [11]. It has also been pointed out that Υ production is an important source of background when $m_{ll} < 12$ GeV. However it is unlikely that the background distribution has a peak at $A_T \gg 0$. A peak of the signal distribution may be observed

[9]Our assumptions of the errors for m_{ll} end points are substantially conservative for those found in literature [5,7].

[10]For point 5, end points of m_{ll}, m_{lq}, m_{llq} distributions in addition to the lower end point of m_{llq} distribution when $m_{ll} > m_{ll}^{\max}/2$ is required to determine $m_{\tilde{\chi}_1^0}$ mass within the $O(10\%)$ model independently [7].

precisely on the top of such backgrounds, especially when signal rates are high enough to allow precision studies. Besides, one only needs to require $m_{ll}<m_{ll}^{\max}/2$ to see structure in the A_T distribution. The peak position that may deviate from A_E^0 could be corrected from the P_T^l distribution in an almost model independent way.

Recently, it was pointed out in [7] that one can obtain the same information by taking the ratio of the end points of the invariant masses of jets and lepton(s). Their analysis was carried out for point 5. The dominant cascade decay process is $\tilde{q}\to\tilde{\chi}_2^0 q$ followed by $\tilde{\chi}_2^0\to\tilde{l}l_1$, and $\tilde{l}\to\tilde{\chi}_1^0 l_2$. Jets from squark decays are substantially harder than the other jets, and can be identified. A correct set of a jet and a lepton pair originating from a squark decay is then selected by requiring that $m_{llj}<600$ GeV for one of the two hardest jets j, and $m_{llj'}>600$ GeV for the other jet j'. The end points of the invariant mass distribution m_{l_1q} and $m_{l_1l_2q}$ are expressed as simple analytical functions of $m_{\tilde{q}}$, $m_{\tilde{l}}$, $m_{\tilde{\chi}_{1(2)}^0}$. One can reconstruct the m_{l_1q} end point by choosing the combination of the first lepton and the jet.[11]

Although each end point is 10%–4% smaller than expectation depending on jet definition, the ratio

$$\frac{m_{lq}^{\max}}{m_{llq}^{\max}}=\sqrt{\frac{m_{\tilde{\chi}_2^0}^2-m_{\tilde{l}}^2}{m_{\tilde{\chi}_2^0}^2-m_{\tilde{\chi}_1^0}^2}}=\sqrt{\frac{1}{1+(A_E^0)^{-1}}} \tag{14}$$

agrees with the expectation.[12] The fitted value ranges from 0.87 ($\Delta R=0.4$ for jet definition) to 0.877 ($\Delta R=0.7$) while the expectation is 0.868. The range corresponds to $A_E^0=0.321$–0.30 while the expectation is 0.327. Our fit gives $A_0=0.324\pm0.009$ for the same point. The comparison of systematics might be an interesting topic for future studies. Our $A_T^{\rm peak}$ analysis may be performed even if jets and leptons in the same cascade decay chain cannot be identified, therefore it can be applied in a wider context.[13]

It is also interesting to reconstruct the kinematics when both $\tilde{\chi}_2^0\to\tilde{l}_R l$ and $\tilde{\chi}_2^0\to\tilde{l}_L l$ are open and the branching ratios are of the same order. In addition to the two edges of the m_{ll} distribution $m_{ll}^{\max}$(low) and $m_{ll}^{\max}$(high), one should be able

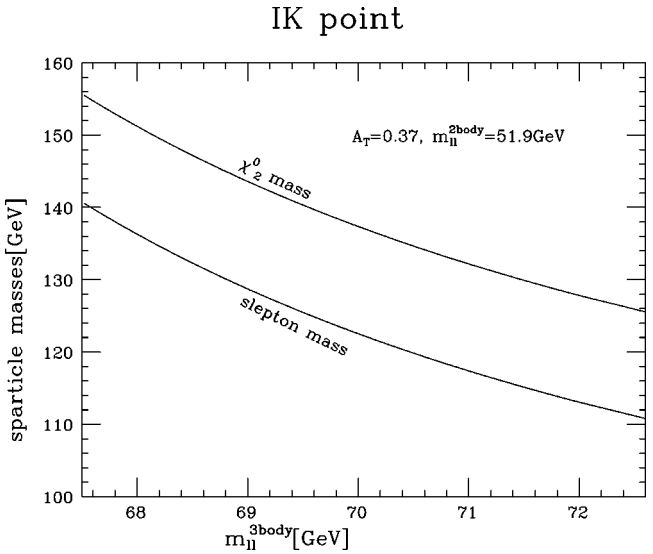

FIG. 15. $m_{\tilde{\chi}_2^0}$ and $m_{\tilde{l}}$ as the function of $m_{ll}^{3\,\rm body}$ when $A_E^0=0.37$ and $m_{ll}^{2\,\rm body}=51.9$ GeV.

to observe two peaks in the A_T distribution, $A_T^{(1)}$ and $A_T^{(2)}$, corresponding to the two decay chains. By comparing A_T distributions for $m_{ll}\lesssim m_{ll}$(low)/2 and m_{ll}(low)/2$<m_{ll}<m_{ll}$(high)/2, one should be able to determine proper sets of the m_{ll} edge and the peak, because the peak at $A_T^{(1)}$ can be hardly observed for $m_{ll}>m_{ll}$(low)/2, while the peak at $A_T^{(2)}$ can still be seen. Note that there are four parameters for four constraints in this case, therefore one can in principle solve for all mass parameters.

V. DISCUSSION

The second lightest neutralino $\tilde{\chi}_2^0$ would be copiously produced from $\tilde{q}$ and $\tilde{g}$ decays at the LHC, and $\tilde{\chi}_1^+\tilde{\chi}_2^0$ production is an important mode for the Tevatron. In this paper, we have studied the distribution of the P_T^l asymmetry, $A_T\equiv P_{T2}^l/P_{T1}^l$, of the lepton-antilepton pair that arises from the cascade decay $\tilde{\chi}_2^0\to\tilde{l}l\to\tilde{\chi}_1^0 ll$. We have found that the A_T distribution shows a clear peak structure in a wide parameter region if $m_{ll}<m_{ll}^{\max}/2$ is required. The peak position is insensitive to the parent $\tilde{\chi}_2^0$ velocity distribution, and in the limit of $m_{ll}\sim0$, it is understood as A_E^0, the ratio of lepton and antilepton energy in the rest frame of $\tilde{\chi}_2^0$. The ratio A_E^0 is a simple function of $m_{\tilde{\chi}_2^0}$, $m_{\tilde{l}}$ and $m_{\tilde{\chi}_1^0}$.

We have also performed MC simulations for several representative points. Values of the peak position obtained by fitting MC data agree with those for $\tilde{\chi}_2^0$ with typical velocity. This follows from the insensitivity of the A_T distribution to the parent neutralino velocity. The typical velocity could be estimated easily by using the hardest lepton P_T distribution. Therefore the A_T peak can be used to constrain $m_{\tilde{\chi}_2^0}$, $m_{\tilde{l}}$ and $m_{\tilde{\chi}_1^0}$. By using the edge of the m_{ll} distribution in addition to the A_T distribution, one can determine two degrees of freedom of the three mass parameters involved in the $\tilde{\chi}_2^0$ cascade

[11]Note that the efficient selection of the first lepton for m_{lq} distribution relies on large lepton energy asymmetry. However as $A\to1$, the end points of m_{l_1j} and m_{l_2j} tend to coincide, therefore it may not be a problem.

[12]When $m_{\tilde{l}}^2-m_{\tilde{\chi}_1^0}^2>m_{\tilde{\chi}_2^0}^2-m_{\tilde{l}}^2$, $m_{lq}/m_{llq}=\sqrt{(m_{\tilde{l}}^2-m_{\tilde{\chi}_1^0}^2)/(m_{\tilde{\chi}_2^0}^2-m_{\tilde{\chi}_1^0}^2)}$.

[13]Another potential problem of the analysis in [7] is that $m_{\tilde{q}}-m_{llj}^{\max}=145$ GeV is almost as small as $m_{\tilde{\chi}_1^0}=122$ GeV, because the end point of the m_{llj} distribution requires the $\tilde{\chi}_1^0$ from the decay chain to be very nonrelativistic in the $\tilde{q}$ rest frame. This should reduce $\not{E}_T$ toward the end point. In general the m_{llj} and m_{lj} end points correspond to different kinematical configurations; attention must be paid to the consequence for relative efficiencies.

decay. When the end point of the m_{ll} distribution of the three body decay $\tilde{\chi}_2^0 \to \tilde{\chi}_1^0 ll$ can be measured simultaneously, one can determine *all* the mass parameters describing $\tilde{\chi}_2^0$ cascade decays. The analysis is entirely based on lepton distributions and does not rely on jet energy measurements.

The reconstruction of the $\tilde{\chi}_2^0$ momentum distribution is of some importance for our analysis. The hardest lepton P_T distribution should allow us to study the $\tilde{\chi}_2^0$ velocity distribution independently from the $\tilde{q}, \tilde{g}$ mass determination. In fact, the measurement of this distribution may allow one to constrain the kinematics of squark and gluino production.

The fit proposed in this paper is reasonably model independent compared to the previous fits using the entire A_T distribution without m_{ll} cuts. It is amazing to see that the distribution keeps the information on the cascade decay kinematics. (Compare Figs. 7 and 10.) The analysis can be extended to all cascade decays involving leptons, such as the gauge mediated scenario with the NLSP slepton [13,6]. The determination of the A_T peak position is not disturbed even in the case where several sleptons contribute to signal lepton pairs.

Note that model independent constraints on weakly interacting sparticle masses may be used to directly constrain the relic mass density of LSPs in our universe. The density of such Big Bang relics is roughly proportional to the inverse of the pair annihilation cross section of the lightest neutralino. In the MSUGRA model, $1/\sigma \sim m_{\tilde{l}}^4 / m_{\tilde{\chi}_1^0}^2$ in the bino dominant limit [14]. If the overall sparticle scale is constrained within 10%, an upper bound on the mass density could be derived within 20%. The improved determination of SUSY parameters at the LHC combined with improved astronomical observations might significantly constrain the remaining MSSM parameters.

In this paper, we did not perform any MC simulation for Tevatron experiments. There the cleanest discovery process is the three leptons and missing $\not{E}_T$ channel of $\tilde{\chi}_1^+ \tilde{\chi}_2^0$ production and decay. It is possible to perform a parallel analysis to the one presented in this paper. However if $m_{ll}^{\max}$ is small (which is likely due to the lower bound on $m_{\tilde{l}}$ of nearly 100 GeV), the number of events that satisfy 12 GeV$< m_{ll} < m_{ll}^{\max}/2$ would be small, where the lower m_{ll} cut is needed to avoid γ^* and Υ backgrounds.

The branching ratio of the mode $\tilde{\chi}_2^0 \to \tilde{l} l$ could be small if other modes such us $\tilde{\chi}_2^0 \to Z, h \ldots$ dominate. The decay $\tilde{\chi}_2^0 \to \tilde{\tau} \tau$ may be the only two body decay channel accessible in the MSUGRA model due to $\tilde{\tau}$ mixing. The analysis would be substantially more difficult for this case, as τ decays further into a jet or a lepton [15]. Selecting two τ leptons which go roughly into the same direction (small ΔR) should effectively work as an $m_{\tau\tau}$ cut in our analysis. However, the A_T distribution of the τ jet would be substantially smeared by the τ decay.

When all two body decay modes are closed, the decay $\tilde{\chi}_2^0 \to \tilde{\chi}_1^0 ll$ often has a sizable branching ratio. The precision study of the three body decay distribution has been discussed in [16]. The m_{ll} distribution and the A_T distribution in the small m_{ll} region would give us information on neutralino mixing and on $m_{\tilde{l}_{L(R)}}$.

It would be interesting to check if our analysis can be extended to other cascade decays involving photons or jets [6]. Note that in the gauge mediated model with $\tilde{\chi}_1^0$ NLSP, the decay chain $\tilde{\chi}_2^0 \to \tilde{\chi}_1^0 ll$ may be associated with a photon from $\tilde{\chi}_1^0 \to \tilde{G} \gamma$ [13]. Cascade decays involving a jet and a lepton or two jets may also be used for an asymmetry analysis, but selecting the proper combination of jets would be challenging.

ACKNOWLEDGMENTS

We thank H. Baer and M. Drees for discussions. We also thank M. Drees for careful reading of the manuscript. M.N. wishes to thank the ITP, Santa Barbara for its support during part of this work (NSF Grant No. PHY94-07194).

[1] For a review, see H. E. Haber and G. L. Kane, Phys. Rep. **117**, 75 (1985).
[2] Proceedings of the 1996 DPF/DPB Summer Study on High-Energy Physics, edited by D. G. Cassel, L. T. Gennari, and R. H. Siemann.
[3] F. Gabbiani and A. Masiero, Nucl. Phys. **B322**, 235 (1989); F. Gabbiani, E. Gabrielli, A. Masiero, and L. Silvestrini, *ibid.* **B477**, 321 (1996).
[4] For a review of minimal supergravity, see H. P. Nilles, Phys. Rep. **110C**, 1 (1984); Some recent developments are M. Dine, A. E. Nelson, Y. Nir, and Y. Shirman, Phys. Rev. D **53**, 2658 (1996); G. Dvali and A. Pomarol, Phys. Rev. Lett. **77**, 3728 (1996); L. Randall and R. Sundrum, Nucl. Phys. **B557**, 79 (1999).
[5] I. Hinchliffe, F. E. Paige, M. D. Shapiro, J. Soderqvist, and W. Yao, Phys. Rev. D **55**, 5520 (1997).
[6] I. Hinchliffe and F. E. Paige, Phys. Rev. D **60**, 095002 (1999).
[7] H. Bachacou, I. Hinchliffe, and F. E. Paige, Phys. Rev. D **62**, 015009 (2000).
[8] I. Iashvili and A. Kharchilava, Nucl. Phys. **B526**, 153 (1998).
[9] M. M. Nojiri, Proceedings of the International Symposium on Supersymmetry, Supergravity and Superstring, Seoul, Korea, 1999, hep-ph/9907530.
[10] F. E. Paige, S. D. Protopopescu, H. Baer, and X. Tata, hep-ph/9810440.
[11] V. Barger and C. Kao, Phys. Rev. D **60**, 115015 (1999); K. Matchev and D. Pierce, *ibid.* **60**, 075004 (1999); K. T. Matchev and D. M. Pierce, Phys. Lett. B **467**, 225 (1999); J. D. Lykken and K. Matchev, Phys. Rev. D **61**, 015001 (2000); H. Baer, M. Drees, F. Paige, P. Quintana, and X. Tata, *ibid.* **61**, 095007 (2000).
[12] E. Richter-Was *et al.*, ATLFAST2.21, ATLAS Internal Note, PHYS-NO-079.

[13] S. Dimopoulos, M. Dine, S. Raby, and S. Thomas, Phys. Rev. Lett. **76**, 3494 (1996); S. Dimopoulos, S. Thomas, and J. D. Wells, Phys. Rev. D **54**, 3283 (1996).

[14] See for example M. Drees and M. M. Nojiri, Phys. Rev. D **47**, 376 (1993); G. Jungman, M. Kamionkowski, and K. Griest, Phys. Rep. **267**, 195 (1996).

[15] H. Baer, C.-H. Chen, M. Drees, F. Paige, and X. Tata, Phys. Rev. D **59**, 055014 (1999); D. Denegri, W. Majerotto, and L. Rurua, *ibid.* **60**, 035008 (1999); I. Hinchliffe and F. E. Paige, *ibid.* **61**, 095011 (2000).

[16] M. M. Nojiri and Y. Yamada, Phys. Rev. D **60**, 015006 (1999).